Sensors and Actuators A 186 (2012) 236–241

Contents lists available at SciVerse ScienceDirect

Sensors and Actuators A: Physical

journal homepage: www.elsevier.com/locate/sna

An array of 100 μm × 100 μm dielectric elastomer actuators with 80% strain for tissue engineering applications

Samin Akbari*, Herbert R. Shea

Microsystems for Space Technologies Laboratory, École Polytechnique Fédérale de Lausanne (EPFL), Rue Jaquet Droz 1, 2002, Neuchâtel, Switzerland

ARTICLE INFO

Article history:
Available online 27 January 2012

Keywords:
Dielectric elastomer actuator
Microactuator
Low energy ion-implantation
Single cell stretcher
Mechanotransduction

ABSTRACT

Biological cells modulate their behavior, express genes, proliferate or differentiate in response to mechanical strains ranging from 1% to 20%. There currently exists no technique to apply strain to many targeted individual cells in a larger culture in order to perform parallelized high throughput testing. Dielectric elastomer actuators (DEAs) are compliant devices capable of generating large percentage strains with sub-second response time, ideally suited by their compliance for cell manipulation. We report an array of 100 μm × 100 μm DEAs reaching up to 80% in-plane strain at an electric field of 240 V/μm. The miniaturized DEAs are made by patterning 100 μm wide compliant ion-implanted gold electrodes on both sides of a 30 μm thick polydimethylsiloxane (PDMS) membrane. We report the important effect of uniaxial prestretch of the membrane on the microactuators' performance; the largest strain is achieved by prestretching uniaxially by 175%. Each actuator is intended to have a single cell adhered to it in order to periodically stretch the cells to study the effect of mechanical stimulation on its biochemical responses. To avoid short-circuiting all the top electrodes by the conductive saline cell growth medium, a 20 μm thick biocompatible PDMS layer is bonded on the actuators. In this configuration, 37% strain is achieved at 3.6 kV with sub-second response. This device can be used as a high throughput single cell stretcher to apply relevant biological periodic strains to individual cells in a single experiment.

1. Introduction

Dielectric elastomer actuators (DEAs) are an emerging class of polymer-based actuators, combining large strains, high energy density and fast response time [1,2]. DEAs consist of a thin elastomeric membrane sandwiched between two compliant electrodes. When a voltage is applied between the electrodes, due to a compressive electrostatic pressure, the membrane is compressed and expands in-plane. DEA devices generally range from cm scale (e.g. compact motors [3], peristaltic pumps [4], see Refs. [5,6] for a review) to meter scale (energy harvesting from ocean waves [7] and airships [8]).

Miniaturization of dielectric elastomer actuators is challenging due to lack of reliable and repeatable methods to pattern μm-scale compliant electrodes. Electrodes in DEAs must not stiffen the elastomer significantly, and must remain conductive at the large actuation strain levels (typically from 3% to 100%). Carbon based electrodes such as carbon grease or carbon powder are commonly used, as are soft and stretchable but very challenging to pattern in micrometer scale. For sub-mm size DEA, Aschwanden and Stemmer have used a polydimethylsiloxane (PDMS) stamp to pattern 100 μm wide carbon powder electrodes on acrylic films (VHB 4910 from 3M) for tunable gratings [9]. Carbon powders easily transfer from the PDMS stamp to the VHB 4910 adhesive film. But using a PDMS stamp to pattern carbon powders on a PDMS membrane is more difficult as the stamp and film have the same surface energies. Silicone films are increasingly preferred to acrylic elastomer films since they have negligible viscoelastic properties and stable dynamic behavior, and longer lifetime [10]. Pimpin et al. have shown buckling mode microactuators using patterned concentric circle metal electrodes on silicone elastomers [11], but these electrodes still have a significant impact on the stiffness of the polymer. Several groups have reported on mm-scale DEA devices. Lotz et al. have sprayed graphite powder to make staked actuators for tactile displays [12] and peristaltic pumps [4]. The Pei group at UCLA has recently shown a refreshable Braille cell [13] based on their bistable electroactive polymer technology [14].

Our group has employed low-energy ion-implantation (<5 keV) to pattern μm to mm sized highly compliant electrodes that can conduct at up to 175% strain, be cycled over 10^5 times, and are cleanroom compatible [15]. The implanted gold forms a 30 nm thick nano-composite that adds very little stiffness to the underlying PDMS [16]. We have used these implanted compliant electrode to fabricate a range of miniaturized DEAs [17], including buckling actuators [18], tunable lenses [19] or tunable acoustic filters [20].

* Corresponding author. Tel.: +41 32 720 5460; fax: +41 32 720 5754.
E-mail address: samin.akbari@epfl.ch (S. Akbari).

0924-4247/$ – see front matter © 2012 Elsevier B.V. All rights reserved.
doi:10.1016/j.sna.2012.01.030

In this work, we have patterned 100 μm wide compliant electrodes by ion-implantation at the energy of 2.5 keV that remain conductive and functional until the device fails at 118% area strain. Two perpendicular arrays of microelectrodes are patterned on top and bottom surfaces of a silicone membrane to fabricate an array of 100 μm × 100 μm microactuators for single cell stretching applications. It is intended to attach individual cells on each actuator to stimulate them with a periodic mechanical strain as the actuators expand in-plane. Currently, most of the cell-stretching devices have cm^2 area, monitoring average response of 100,000 of cells at the same time (refer to the review by Brown [21]). However, to precisely understand how cells decipher the mechanical strain and evoke a biochemical response, devices are required to stretch single cells. There are few silicon based MEMS devices that can apply precise and calibrated strain to only one cell in one experiment [22,23] as reviewed by Desmaële et al. [24]. These devices have a low throughput and require multiple experiments over several days to test the effect of various strain levels or frequencies that leads to unconfident results. We aim to make a high throughput single cell stretching device which is not yet developed based on electroactive polymers.

We have previously reported the design principle [25], and microfabrication and characterization of an array 100 μm × 200 μm DEA actuators generating up to 5% uniaxial strain for single cell stretching [26]. That first generation of devices consisted of a non-prestretched PDMS membrane bonded to a Pyrex chip with 200 μm wide trenches to ensure uniaxial deformation. Strains were however limited to 5%, lower than needed to address the full range of cells. We report here a second generation of devices, based on a suspended uniaxially prestretched PDMS membrane, allowing much larger strains. In this paper, the fabrication and characterization of the array of 100 μm × 100 μm actuators are presented. The effect of prestretch ratio on the actuator's performance is investigated. 80% in-plane strain on a 175% uniaxially prestretched membrane is achieved. To make the actuators compatible with cell stretching application, actuators are fabricated with an additional 20 μm thick passive PDMS layer, to avoid short-circuiting of the top electrode due to the conductive cell culture medium. 37% strain was achieved with these devices.

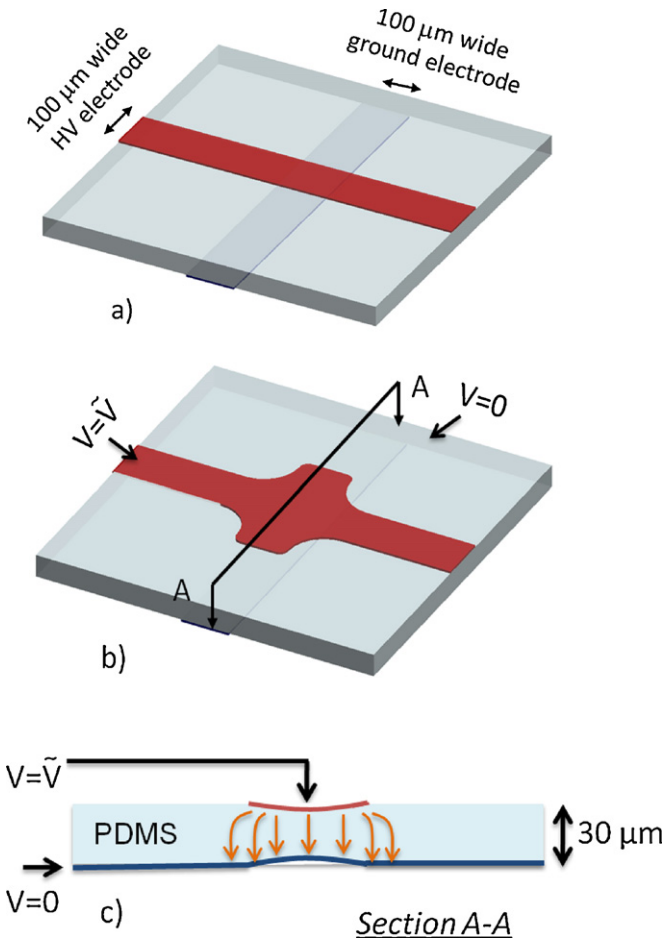

Fig. 1. Operating principle of a dielectric elastomer microactuator: (a) Two perpendicular compliant microelectrodes are patterned on top and bottom layers of a thin PDMS membrane. (b) A high voltage is applied between the electrodes, squeezing the membrane in thickness and expanding it in-plane. (c) Cross section view of the actuator in the actuated state, showing the electric field at the intersection of the electrodes and the fringe fields as the aspect ratio of the electrodes' width to its thickness is about 3.

2. Actuation principle

In this section, the operating principle of a dielectric elastomer microactuator and the modifications required for cell stretching applications are explained.

Our dielectric elastomer microactuator consists of a thin soft PDMS membrane. Two perpendicular compliant microelectrodes are patterned on top and bottom layers of the membrane as shown in Fig. 1. When a high voltage is applied between the electrodes, at the intersection of the electrodes, the membrane is squeezed in thickness due to the Maxwell stress and expands in-plane since it is incompressible.

The dielectric elastomer actuators are generally modeled by applying a pressure equal to the Maxwell stress to the electrodes. The Maxwell stress increases quadratically with the applied electric field.

$$P = \varepsilon E^2 \quad (1)$$

where P is the electrostatic pressure, ε is the permittivity and E is the electric field.

Scaling the dielectric elastomer actuator to micro scale, the electrodes dimensions become comparable to the elastomer's thickness, hence assuming parallel electric field in the elastomer is erroneous. In this case, fringe field should be taken into account in the modeling. We compared simulations of the actuators with (a) a voltage applied to the electrodes and (b) no voltage and instead a mechanical pressure equal to the Maxwell stress derived for parallel electric field from Eq. (1) applied to the electrodes. The FEM simulations predicts 13% higher strain at the center of 100 μm × 100 μm actuator on a 30 μm thick PDMS membrane for the full model including fringe fields compared to the assumption of constant parallel electric field.

The actuators are fabricated on uniaxially prestretched membranes. Prestretching the elastomeric polymer has a significant influence on the performance of the actuators such as the actuation strain [2,27]. We report the effect of uniaxial prestretch on the performance of our 100 μm × 100 μm actuators in Section 4.1.

The cells will be attached on top of each actuator by patterning a cell adherent extracellular matrix using micro-contact printing [28]. The objective is to have actuators generating up to 20% strain in order to cover the desired strain levels to stimulate most cell types [29].

To avoid stimulating the cells with high electric field, the high voltage will be applied to the bottom electrode and the top electrode will be grounded. The cells must be kept in the conductive cell culture medium, which will be grounded. If the cell culture medium is directly applied on the active membrane, the possible electric field reaching the cells through the air will be ruled out, but the top

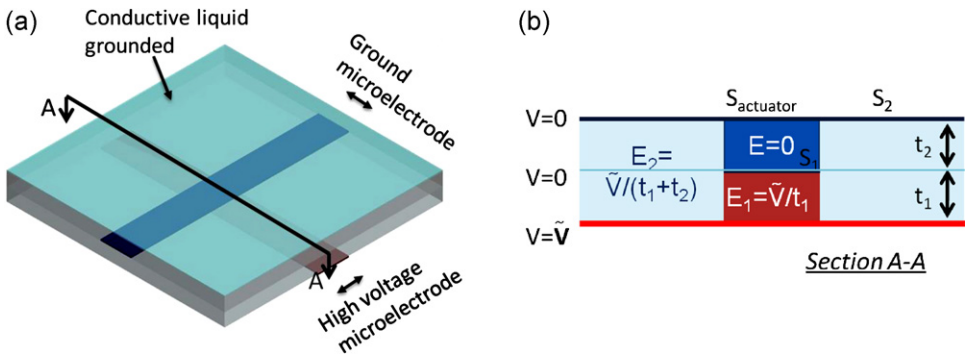

Fig. 2. Modified double-layer actuators for cell stretching applications; (a) A thin layer of PDMS is coated on top of the actuators to avoid short circuit of the ground electrode due to the conductive cell culture medium. (b) Cross section view of the actuator along the high voltage electrode, showing three different zones of electric field.

ground electrodes of the actuator will also short-circuit, resulting in 100 μm × 1 cm actuators instead of 100 μm × 100 μm actuators.

To solve this, another PDMS layer (with comparable thickness to the actuator) is bonded on top of the actuators as shown in Fig. 2a. The high voltage is applied to the bottom microelectrode, the perpendicular microelectrode is grounded and the top layer of the second PDMS layer is also grounded by the conductive liquid. This leads to three different zones of electric field inside the elastomer along the high voltage electrode, neglecting the fringe field effect, as illustrated in Fig. 2b. At the intersection of the electrodes, the electric field is maximum in the first PDMS layer ($E_1 = V/t_1$) and is zero in the second layer. The electric field elsewhere along the high voltage electrode is E_2 which is equal to $E_1 t_1/(t_1 + t_2)$. Therefore, the electrostatic stress at the intersection of the electrodes in the first layer is $(t_1 + t_2)^2/t_1^2$ times higher than electrostatic stress along the high voltage electrode (Eq. (1)). Since the force on the active layer due to E_1 has to deform both active and passive layers, the strain on the actuator ($S_{actuator}$) is $(t_1 + t_2)/t_1$ times higher than the strain elsewhere along the electrode (S_2), considering small deformation and constant Young's modulus. We will show later in Section 4.2, that in the case of large deformations in our actuators with 80% strain, due to the hyperelastic stress–strain relationship and thickness reduction of PDMS membrane, much higher ratios of $S_{actuator}/S_2$ is obtainable compared to the simple small deformations model. Therefore, adding a passive layer on top of the actuators leads to the dominant strain on the 100 μm × 100 μm actuators while allowing operation in conductive liquid.

3. Fabrication

3.1. Fabrication of single-layer actuators

First, a thin film of PDMS membrane is prepared. Two components of Sylgard 186 from Dow Corning are mixed with 10:1 weight ratio as recommended by the manufacturer, and diluted with iso-octane (PDMS:Solvent 10:9 weight) in order to decrease its viscosity. The mixture is degassed for 30 min until all the trapped air bubbles are released. A universal applicator ZUA 2000 from Zehntner GmbH Testing Instruments is used to cast the PDMS mixture on a 55 μm thick polyimide film as a support. The parameters are adjusted to have several films with thicknesses ranging from 30 μm to 60 μm after curing at 100 °C for 40 min in the oven. To avoid having dust particles in the membrane which will decrease the break down voltage, the process is performed in a clean environment. The films are then uniaxially stretched from 0 to 2.75 times of their initial lengths and transferred to a frame with help of a double sided adhesive. The initial thickness of the films was varied in order to keep the final thickness of the stretched membrane at 30 μm.

Two arrays of perpendicular 100 μm wide electrodes are patterned on top and bottom surfaces of the PDMS membrane. To have compliant electrodes, low energy ion-implantation is employed. A filtered cathodic vacuum arc source is used to sputter the gold ions from a 3 mm diameter gold source and implant them inside the PDMS membrane. This leads to clusters of gold nanoparticles in depth of 20–50 nm of PDMS membrane that create a conductive path [15,16]. Low-energy ion-implantation has a low impact on the Young's modulus of the PDMS membrane (<40% increase) at resistivity of around 1 kΩ/□ which is sufficient for actuation of dielectric elastomer actuators. The other privilege of using ion-implanted compliant electrodes compared to carbon based compliant electrodes is their μm-scale patternablility. We have previously shown that to decrease the shadowing effect and charge trapping in the mask, a conductive mask thinner than the electrode's size should be used [26]. Hence, a 70 μm thick stainless steel mask is used to pattern arrays of 100 μm wide electrodes on the stretched suspended PDMS membrane at the energy of 2.5 keV. The ion dose is chosen slightly higher than the percolation threshold to have electrodes with resistivity of around 1 kΩ/□ with 40% higher Young's modulus than the non-implanted PDMS. A thin layer of gold is deposited using a sputter coated at the outer edges of the 100 μm wide electrodes, and thin wires are connected to the microelectrodes with a conductive tape in order to connect to a high-voltage supply.

Fig. 3 shows four 100 μm × 100 μm actuators of the array of nine actuators. The bright lines are the ion-implanted electrodes on top and the perpendicular dark lines are the electrodes on the bottom layer of the membrane. The actuators are at the intersection

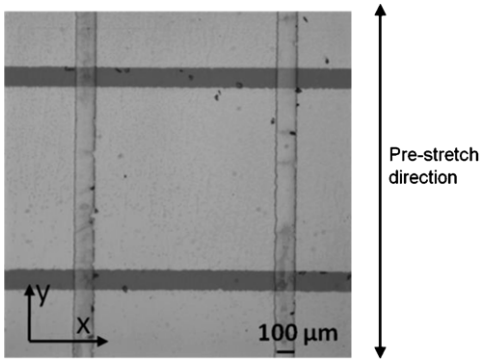

Fig. 3. Top view of a portion of a single-layer device showing four actuators. The bright horizontal lines are the 100 μm wide ion implanted electrodes on the top side of the PDMS membrane and the dark vertical lines are the bottom electrodes. The actuators, where the electrostatic pressure is applied, are at the intersection of the electrodes.

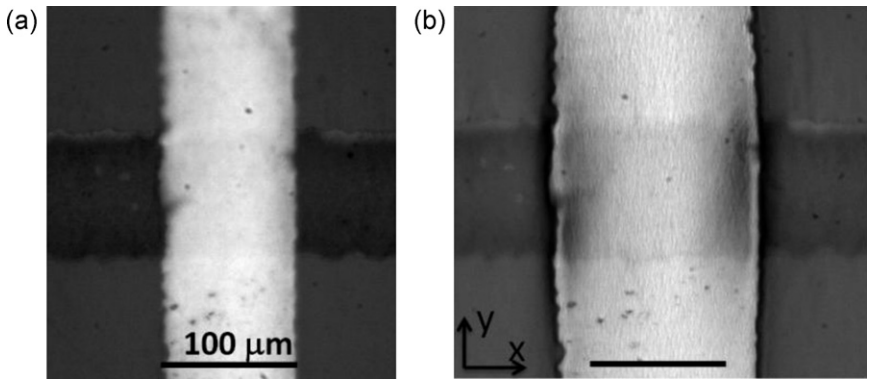

Fig. 4. (a) Optical micrograph of a single-layer microactuator at zero volts at 20× magnification. The membrane is pre-stretched by 175% along the *y*-axis. (b) With 3.8 kV applied between the two electrodes, the membrane expands by 56% along the *x*-axis.

of the electrodes, where the electric field squeezes the membrane in thickness leading to in-plane expansion.

3.2. Fabrication of double-layer actuators

First, a single-layer device is made on a 160% uniaxially pre-stretched membrane. Then, the electrical contacts at the outer edges of the electrodes on the top layer is protected with a 25 μm thick Teflon film (PFA from Dupont) and a 20 μm thick PDMS layer is spray coated on top using an airbrush with a tip diameter of 300 μm. The PDMS mixture is highly diluted (PDMS:Solvent 1:3 weight) to be able to spray coat it. Then, the Teflon films are removed and the PDMS layer is cured in the oven at 60 °C for 4 h. Higher curing temperatures should be avoided: (1) to not lose the conductivity of the electrodes due to different thermal expansions of the PDMS and gold, and (2) to not tear the highly prestretched membrane due to the extra stress caused by shrinkage of the liquid PDMS or the thermal stress during curing.

4. Characterization

In this section, four different single-layer actuators with uniaxial prestretch levels ranging from 0% to 175% are tested and their in-plane actuation strain with respect to the applied electric field is characterized. Then a double-layer actuator compatible with cell stretching application is characterized showing up to 37% strain.

4.1. Characterization of single-layer actuators

To characterize the in-plane strains of the microactuators, microscope images are recorded for different actuation voltages. The widths of the electrodes before and after actuation are compared with the ImageJ software [30]. The displacement field is assumed to be linear and the relative strain is calculated by dividing the electrode's width increase to the initial width. The strain levels discussed in this paper are all relative as the prestrain is not considered in the calculation. Fig. 4, shows the optical micrograph of a 100 μm × 100 μm actuator made on a PDMS membrane initially 175% prestretched in *y* direction. The large expansion of the electrode is clearly observed in Fig. 4b at 3.8 kV. The *x*-axis and *y*-axis strain are measured by detecting edges of the top electrode and the bottom electrode, respectively.

The *x*-axis strain of different actuators with four different prestretch levels versus the applied electric field is plotted in Fig. 5. The applied voltage is increased till the actuators fail. The failure mode of the actuators can stem from (a) rupture of the membrane due to exceeding the mechanical limit of the PDMS (b) exceeding the breakdown electric field of PDMS membrane, or (c) the pull-in instability which will lead to failure mode a or b. Uniaxially pre-stretching the membrane enhances the maximum actuation strain: up to 80% strain is generated on a film with 175% prestretch level, while only 7.7% strain is obtained for 0% prestretch. It bears noting that the sustainable electric field of the PDMS membrane has also significantly increased.

To calculate the electric field at large deformations, the thickness reduction of the membrane must be considered. We have calculated the thickness at each voltage step from the in-plane strains and assumed incompressibility for the elastomer.

$$\lambda_x \lambda_y \lambda_z = 1 \tag{2}$$

where λ_i is the stretch ratio along the i direction ($i = x, y, z$) and is equal to 1 + strain$_i$. The reference state for strain calculation is the prestretched state. Thus, the true electric field can be computed as

$$E = \frac{V\lambda_x\lambda_y}{t_0} \tag{3}$$

where t_0 is the initial thickness of the films after prestretching and V is the applied voltage.

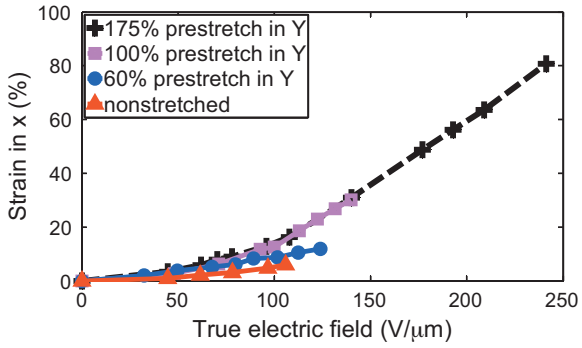

Fig. 5. The *x*-axis strain of the single-layer actuator versus the true electric field. The PDMS membrane is pre-stretched uniaxially along the *y*-axis. The *x*-axis strain is increased up to 80% by pre-stretching the membrane 175% in the *y*-axis.

Table 1
Effect of uniaxial prestretch level on performance of the microactuators. There is 0% prestretch on the *x*-axis.

Prestretch level along *y*-axis (%)	Maximum strain in *x* (%)	Strain$_x$/Strain$_y$	Maximum sustainable electric field (V/μm)
0	7.7	1	106
60	14.5	1.2	124
100	29.2	2	140
175	80.7	5.6	241

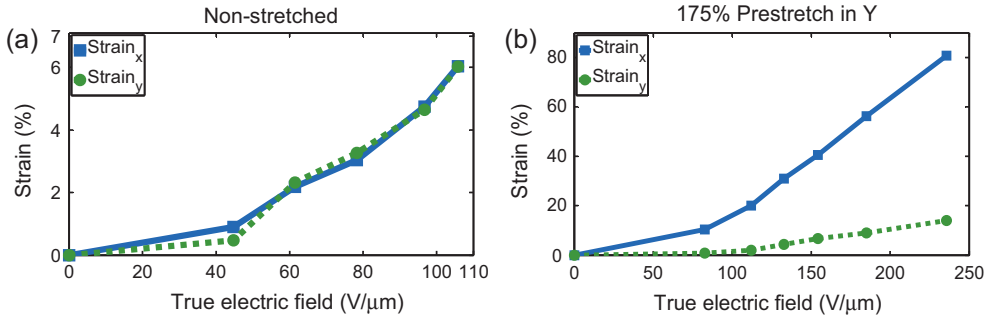

Fig. 6. Actuated strains in the *x* and *y* direction versus the true electric field for a single-layer actuator. (a) Non-stretched membrane. (b) The membrane is prestretched by 175% along the y direction. The ratio of *x*- to *y*-axis strains is tunable by adjusting the prestretch level in *x* and *y* directions.

The *x*- and *y*-axis actuated strains of the microactuator on a non-stretched PDMS membrane are equal as shown in Fig. 6a, while an anisotropic actuation strain is observed on 175% uniaxially prestretched actuator, as plotted in Fig. 6b. Due to hyperelastic behavior of PDMS, uniaxial prestretching leads to anisotropic stiffness of the membrane. Therefore, the membrane expands less along the prestretched direction, which is stiffer. The ratio of *x*-axis strain to the *y*-axis strain of the actuators at their maximum sustainable electric field is listed in Table 1. The ratio of the strain in *x* to strain in *y* direction is increased up to 5.6 with 175% uniaxial prestretch. Therefore, purely biaxial or semi-uniaxial stretchers can be made by introducing isotropic or anisotropic prestretch in the elastomer.

The effect of uniaxial presstretching on performance of the microactuators is summerized in Table 1. The sustainable electric field and the strain level are enhanced by prestretching as the pull-in instability occurs at higher strains [31] when in the hyperelastic regime.

4.2. Characterization of double-layer actuators

As described in Section 2, in order to use the abovementioned actuators for cell stretching applications, a 20 μm thick PDMS layer is bonded on the actuators to avoid short-circuiting of the top microelectrodes in the conductive cell growth medium which would lead to actuation over the full length of the electrode and not only at the intersection of the top and bottom electrodes. The passive layer enables having the dominant strain at the 100 μm × 100 μm electrode intersection area, especially at large deformations. In Fig. 7, the *x*-axis strain of one actuator on a 175% uniaxially prestretched membrane is plotted versus the nominal electric field, which is the applied voltage divided by the initial thickness. Assuming the same thickness for the passive layer, when

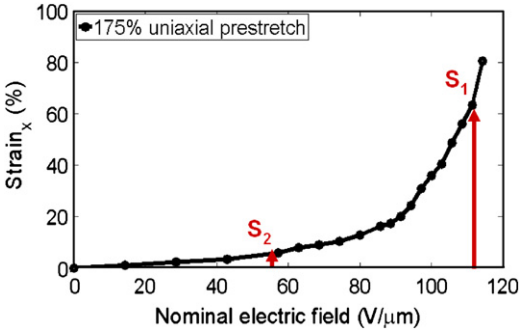

Fig. 7. *x*-Axis strain of a single-layer 100 μm × 100 μm actuator versus the nominal electric field on a 175% uniaxially prestretched membrane. The arrows show the strain on 100 μm × 100 μm area in the first layer (S_1) and elsewhere along the high voltage electrode (S_2), assuming the same thickness for both PDMS layers (refer to Fig. 2 for S_1 and S_2).

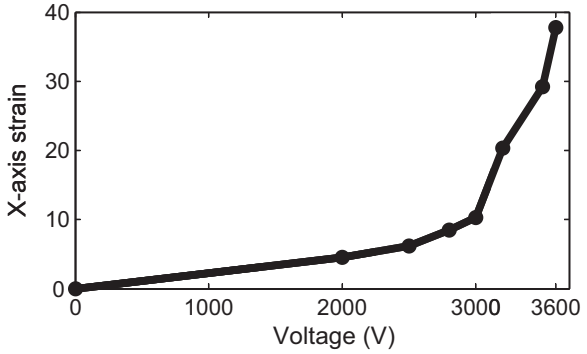

Fig. 8. *x*-Axis strain of a double-layer 100 μm × 100 μm actuator versus the applied voltage, showing up to 37% relative strain. The first layer is uniaxially prestretched 160%, thickness of the stretched membrane is 34 μm after prestretching and thickness of the coated passive layer is 20 μm.

the electric field at the intersection of the electrodes in the first layer (E_1, shown Fig. 2b) is 111 V/μm resulting in 63% strain, the electric field elsewhere along the high voltage electrode (E_2) is 55.5 V/μm generating only 5% strain. As the electrostatic force on the active layer should stretch both passive and active layers, the final strain on the 100 μm × 100 μm is half of the strain generated in the active layer (31.5%), which is still 6.3 times more than the strain elsewhere along the electrode. The small deformation calculations presented in Section 2, predicts only 2 times higher strain.

The relative *x*-axis strain of the two-layer actuator fabricated with 20 μm thick passive layer versus the applied voltage is plotted in Fig. 8. Up to 37% in-plane strain is achieved at 3.6 kV. As these actuators have sub-second response time, they are able to stimulate all cell types with relevant biological strain and frequencies. As the next step, the performance and lifetime of the actuators in conductive liquids will be tested, followed by biological experiments with adhered cells.

5. Conclusion

We have developed an array of 100 μm × 100 μm dielectric elastomer actuators generating up to 80% in-plane strain. The compliant 100 μm wide electrodes patterned by gold ion-implantation remain conductive and functional up to 118% area strain, at which point the actuators fail. Low energy ion-implantation is a very effective method to pattern compliant microelectrodes, addressing the lack of suitable fabrication techniques to pattern μm scale electrodes on silicone membranes.

Uniaxial prestretch in the silicone films enables large deformation on the microactuators by retarding the pull-in instability and allowing higher electric fields before failure. It also results in

anisotropic strain field as it stiffens the polymer in the stretched direction.

The array of microactuators is designed to stretch single cells attached on top of them in order to study the mechanotransduction in single cell level. To avoid short-circuiting the top microelectrode in the conductive cell culture medium, a passive biocompatible PDMS layer is bonded on top. In this configuration, up to 37% in-plane strain is achieved at 3.8 kV with sub-second response time, which adequately meets the desired strain levels and frequencies for stimulating all cell types. This device as a high throughput single cell stretcher can apply various strain levels to groups of individual cells in one experiment, in order to reveal how the cells modulate their behavior in response to the mechanical strain.

Acknowledgments

We gratefully acknowledge financial support from the Swiss National Science Foundation grant #200020-130453, thank Dr. A. Franco-Obregon from the ETHZ Space Biology Group for helpful advice on cell mechanobiology, and Dr. S. Rosset for helpful discussions. We acknowledge the SNF R'Equip program for the funding of the high speed data acquisition test bench for Microsystems, (RF) MEMS and NEMS used in this study. Support from COST (European Cooperation in Science and Technology) in the framework of ESNAM (European Scientific Network for Artificial Muscles) – COST Action MP1003 – is acknowledged.

References

[1] S. Ashley, Artificial muscles, Scientific American 289 (2003) 52–59.
[2] R. Pelrine, R. Kornbluh, Q. Pei, J. Joseph, High-speed electrically actuated elastomers with strain greater than 100%, Science 287 (2000) 836–839.
[3] I. Anderson, T. Hale, T. Gisby, T. Inamura, T. McKay, B. O'Brien, et al., A thin membrane artificial muscle rotary motor, Applied Physics A: Materials Science & Processing 98 (2010) 75–83.
[4] P. Lotz, M. Matysek, H.F Schlaak, Peristaltic pump made of dielectric elastomer actuators, in: Proceeding of SPIE, San Diego, 2009, pp. 72872D–72881D.
[5] P. Brochu, Q. Pei, Advances in dielectric elastomers for actuators and artificial muscles, Macromolecular Rapid Communications 31 (2010) 10–36.
[6] F. Carpi, D.D. Rossi, R. Kornbluh, R. Pelrine, P.R. Sommer-Larsen, Dielectric Elastomers as Electromechanical Transducers, Elsevier Ltd, Amsterdam, 2008, ISBN 13: 978-0-08-047488-5.
[7] R.D. Kornbluh, R. Pelrine, H. Prahlad, A. Wong-Foy, B. McCoy, S. Kim, et al., From boots to buoys: promises and challenges of dielectric elastomer energy harvesting, in: Proceeding of SPIE, San Diego, California, USA, 2011, pp. 797605–797619, doi:10.1117/12.882367.
[8] C. Jordi, A. Schmidt, G. Kovacs, S. Michel, P. Ermanni, Performance evaluation of cutting-edge dielectric elastomers for large-scale actuator applications, Smart Materials and Structures 20 (2011) 075003.
[9] M. Aschwanden, A. Stemmer, Low voltage, highly tunable diffraction grating based on dielectric elastomer actuators, in: Proceeding of SPIE, San Diego, California, USA, 6524, 2007, doi:10.1117/12.713325, pp. 65241N-10.
[10] M. Molberg, Y. Leterrier, C.J.G. Plummer, C. Walder, C. Löwe, D.M. Opris, et al., Frequency dependent dielectric and mechanical behavior of elastomers for actuator applications, Journal of Applied Physics 106 (2009) 054112–54117.
[11] A. Pimpin, Y. Suzuki, N. Kasagi, Microelectrostrictive actuator with large out-of-plane deformation for flow-control application, Journal of Microelectromechanical Systems 16 (2007) 753–764.
[12] P. Lotz, M. Matysek, H.F. Schlaak, Fabrication application of miniaturized dielectric elastomer stack Actuators, IEEE/ASME Transactions on Mechatronics 16 (2011) 58–66.
[13] X. Niu, P. Brochu, B. Salazar, Q. Pei, Refreshable tactile displays based on bistable electroactive polymer, in: Proceeding of SPIE, San Diego, California, USA, 2011, pp. 797610–797616, doi:10.1117/12.880185.
[14] Z. Yu, W. Yuan, P. Brochu, B. Chen, Z. Liu, Q. Pei, Large-strain, rigid-to-rigid deformation of bistable electroactive polymers, Applied Physics Letters 95 (2009), 192904-1-4.
[15] S. Rosset, M. Niklaus, P. Dubois, H.R. Shea, Metal ion implantation for the fabrication of stretchable electrodes on elastomers, Advanced Functional Materials 19 (2009) 470–478.
[16] M. Niklaus, H.R. Shea, Electrical conductivity and Young's modulus of flexible nanocomposites made by metal-ion implantation of polydimethylsiloxane: the relationship between nanostructure and macroscopic properties, Acta Materialia 59 (2011) 830–840.
[17] H. Shea, Miniaturized EAPs with compliant electrodes fabricated by ion implantation, in: Proceeding of SPIE, San Diego, California, USA, 7976, 2011, doi:10.1117/12.882212, pp. 79760R-1-9.
[18] S. Rosset, M. Niklaus, P. Dubois, H.R. Shea, Large-stroke dielectric elastomer actuators with ion-implanted electrodes, Journal of Microelectromechanical Systems 18 (2009) 1300–1308.
[19] M. Niklaus, S. Rosset, P. Dubois, H. Shea, Ion-implanted compliant electrodes used in dielectric electroactive polymer actuators with large displacement, Procedia Chemistry 1 (2009) 702–705.
[20] P. Dubois, S. Rosset, M. Niklaus, M. Dadras, H. Shea, Voltage control of the resonance frequency of dielectric electroactive polymer (DEAP) membranes, Journal of Microelectromechanical Systems 17 (2008) 1072–1081.
[21] T.D. Brown, Techniques for mechanical stimulation of cells in vitro: a review, Journal of Biomechanics 33 (2000) 3–14.
[22] N. Scuor, P. Gallina, H.V. Panchawagh, R.L. Mahajan, O. Sbaizero, V. Sergo, Design of a novel MEMS platform for the biaxial stimulation of living cells, Biomedical Microdevices 8 (2006) 239–246.
[23] D.B. Serrell, T.L. Oreskovic, A.J. Slifka, R.L. Mahajan, D.S. Finch, A uniaxial bioMEMS device for quantitative force-displacement measurements, Biomedical Microdevices 9 (2007) 267–275.
[24] D. Desmaële, M. Boukallel, S. Régnier, Actuation means for the mechanical stimulation of living cells via microelectromechanical systems: a critical review, Journal of Biomechanics 44 (2011) 1433–1446.
[25] S. Akbari, M. Niklaus, H. Shea, Arrays of EAP micro-actuators for single-cell stretching applications, in: Proceeding of SPIE, San Diego, CA, USA, 7642, 2010, doi:10.1117/12.847125, pp. 76420H-1-10.
[26] S. Akbari, H. Shea, Microfabrication and characterization of an array of dielectric elastomer actuators generating uniaxial strain to stretch individual cells, Submitted to Journal of Micromechanics and Microengineering.
[27] R.D. Kornbluh, R. Pelrine, Q. Pei, S. Oh, J. Joseph, Ultrahigh strain response of field-actuated elastomeric polymers, in: Proceeding of SPIE, Newport Beach, CA, USA, 2000, pp. 51–64.
[28] L. Kam, S.G. Boxer, Cell adhesion to protein-micropatterned-supported lipid bilayer membranes, Journal of Biomedical Materials Research 55 (2001) 487–495.
[29] J. Wang, B. Thampatty, An introductory review of cell mechanobiology, Biomechanics and Modeling in Mechanobiology 5 (2006) 1–16.
[30] http://rsbweb.nih.gov/ij/.
[31] S.J.A. Koh, T. Li, J. Zhou, X. Zhao, W. Hong, J. Zhu, et al., Mechanisms of large actuation strain in dielectric elastomers, Journal of Polymer Science Part B: Polymer Physics 49 (2011) 504–515.

Biographies

Samin Akbari holds a B.Sc. (2005) in mechanical engineering from University of Tehran, Iran and a M.Sc. (2007) in mechanical engineering from Sharif University of Technology, Tehran, Iran. During her master thesis, she developed a novel compliant nano-manipulator capable of positioning in six degrees of freedom. From 2009, she is working toward her Ph.D. program in micro-engineering at École Polytechnique Fédérale de Lausanne (EPFL), Switzerland. She is developing an array of electroactive polymer microactuators for cell manipulation. Her research interests are electroactive polymers microactuators, and MEMS devices for cell stimulation.

Herbert Shea holds a Ph.D. (1997) in physics from Harvard University. After a postdoc in carbon nanotube electronics at IBM's T.J. Watson Research Center in Yorktown Heights, NY, he joined Lucent Technologies' Bell Labs in Murray Hill, NJ, where he became the technical manager of the Microsystems Technology group, specializing in MEMS reliability. In 2004 he founded the Microsystems for Space Technologies Laboratory at the EPFL in Switzerland, where he is currently an associate professor. Current interests include micromachined polymer actuators, electric propulsion and MEMS sensors for small spacecraft, chip-scale plasma sources, and picosatellites.